TRABAJO DE FIN DE GRADO:

Measurements and analysis of optical properties of materials with technological interest

Junio de 2014

Autora:

Lucía Labrador Páez

Tutor:

Inocencio R. Martín Benenzuela

Grado en Física

Universidad de La Laguna

Index

Abstract 2

Aim of this work 3

Introduction 4

Methodology 8

- Experimental procedures 8
- Theoretical models 9
  - Fluorescence intensity ratio technique 9
  - Sensitivity 10
  - Energy transfer processes 10

Results 13

- Temperature dependence of the whispering gallery modes 13
  - Thermalization effect in Er^{3+} ions 15
  - Displacements of the Whispering Gallery Modes 17
- Heating using a microsphere as a focusing lens 19
- Determination of the optimum concentration of doping ion 21

Conclusions 25

References 27

Abstract

Las propiedades ópticas de algunos materiales hacen posible su uso en el desarrollo de sensores ópticos de temperatura. Por ejemplo, algunos iones lantánidos, como el Er^{3+} y el Nd^{3+}, tienen niveles de energía cuya distribución de población varía con la temperatura y que, al mismo tiempo, emiten de forma radiativa. Además, si a partir de un material dopado con esos iones se fabrican microesferas, el número de aplicaciones aumenta considerablemente.

Las microesferas son cavidades resonantes de forma esférica, habitualmente formadas por materiales dieléctricos transparentes y suelen tener diámetros del orden de micras. Deben tener un índice de refracción más alto que el medio que las rodea para producir reflexiones internas en la cavidad y, en consecuencia, los modos resonantes. Posibles cambios en la temperatura pueden provocar la dilatación de la esfera, lo que haría cambiar las dimensiones de la cavidad resonante y su índice de refracción. En consecuencia, variaría la longitud de onda de los modos resonantes.

Las dimensiones de las microesferas y las posibilidades que ofrecen para la transmisión de los datos medidos de forma inalámbrica e, incluso, a través del vacío, son unas de las principales ventajas de su uso como sensores ópticos de temperatura.

Cuando incide radiación sobre una microesfera, ésta puede ser concentrada en una pequeña región a la salida. En determinadas condiciones, tiene una anchura por debajo del límite de difracción de Abbe. En este caso, este fenómeno suele denominarse photonic nanojet. Al actuar la microesfera como una lente, se logra reducir la zona donde incide la luz a la salida de ésta y, por lo tanto, puede provocar un mayor calentamiento del medio sobre el que la esfera está depositada. En la literatura se pueden encontrar aplicaciones para microesferas actuando como lentes tanto en nanotecnología como en investigación en diversos campos de la biología.

Si se desea maximizar la intensidad de la emisión de una muestra dopada con alguno de los iones antes mencionados, se deben estudiar los procesos de transferencia de energía entre iones que tienen lugar en la muestra en función de la concentración del ion dopante. Se debe tener en cuenta que para concentraciones altas los procesos de migración entre iones donores también pueden ser importantes debido a que la distancia entre iones disminuye al aumentar la concentración. Del análisis de estos resultados, se obtendría la concentración de ion dopante óptima para obtener la máxima intensidad de emisión posible.

Aim of this work

El objetivo de este trabajo es analizar la termalización de ciertos niveles del Er^{3+} y del Nd^{3+}, observar el desplazamiento con la temperatura de los modos de resonancia en una microesfera, utilizar microesferas como lentes que concentran la radiación y determinar la concentración de Nd^{3+} que optimizará la emisión de la muestra dopada.

The purpose of this work is to analyse the optical properties of some trivalent lanthanide doped materials. In particular, this work is intended to the following:

- To characterize the thermalization effect in the emission of erbium ions by means of the fluorescence intensity ratio technique.
- To observe the whispering gallery modes yielded by a spherical microresonator consisting of a glass doped with erbium ions.
- To analyse the temperature dependence of whispering gallery modes.
- To compare the temperature dependence of the wavelength of the whispering gallery modes with the thermalization effect in the emission of erbium ions in order to decide which of these methods is more sensitive to temperature shifts.
- To characterize the thermalization effect in the emission of neodymium ions by means of the fluorescence intensity ratio technique.
- To determine the appropriate dimensions of microspheres in order to achieve the maximum concentration of the incident radiation using the nanojet spot.
- To use a microsphere located over a neodymium-doped phosphate glass so as to optimise the heating effect.
- To obtain the optimum concentration of neodymium as doping ion in a phosphate glass in order to attain the highest possible intensity.

Introduction

El desarrollo de sensores ópticos de temperatura aprovechando la termalización de niveles en iones lantánidos como Er^{3+} y Nd^{3+} es un campo de estudio de gran interés en espectroscopía hoy en día. Además, el uso de microesferas dopadas con esos iones cuenta con un gran número de aplicaciones, tanto en ámbitos biológicos como en el desarrollo de tecnología. Las microesferas actúan como cavidades resonantes. La variación de la temperatura provoca la dilatación de la esfera y, en consecuencia, el desplazamiento en longitud de onda de los modos resonantes. Por otra parte, una microesfera puede concentrar la radiación incidente en el nanojet. Si dicho nanojet es focalizado sobre un material, se puede producir un gran calentamiento del mismo en esa zona. Por este motivo, se puede decir que las microesferas actúan también como microlentes. Con el fin de optimizar la emisión de una muestra dopada, se deben estudiar los procesos de transferencia de energía que tienen lugar en función de la concentración del ion dopante. Así, se obtendría la concentración idónea.

The optical properties of some materials enable their study by means of spectroscopic techniques. Chemical elements which have luminescence properties, such as fluorescence emissions, are frequently employed as dopants in order to make possible the study of the host material. The use of lanthanide elements such as Er^{3+}, Yb^{3+} and Nd^{3+} as doping ions has the advantage that they are efficient emitters, even if they are compared with other fluorescent materials [1].

Recently, there has been a growing need of new measuring methods in the fields of nanotechnology and biotechnology. This has influenced research lines in the areas of photonics and spectroscopy and has also promoted the development of new concepts of sensors based on luminescence properties of the materials: the optical sensors [2]. These ones take advantage of the thermally induced changes in the spectral characteristics of the light emitted by ions, such as intensity, phase, polarization, wavelength, lifetime and band shape. In this way, new optical sensor systems are been studied, for instance, those consisting of triply ionized lanthanide ions doped materials [3-7].

The basis of conventional solid state temperature sensors were principally thermoelectric materials (for instance, thermistors and thermocouples). Optical sensors have noticeable advantages if their properties are compared with those of the conventional sensors: greater sensitivity, freedom from electromagnetic interference,

electrical passiveness, wide dynamic range, point and distributed configurations and multiplexing capabilities [8].

Another of the advantages of this type of temperature sensor is that the detection can be made distantly through a transparent medium, allowing even the transmission of the measured signal through the vacuum. On the other hand, it could be a disadvantage that is necessary a spectral analysis so as to obtain the data if this type of sensors is employed.

With respect to use of triply ionized lanthanide ions doped materials, if the precursor material is doped with Er^{3+}, changes in the shapes of some of their emission bands due to thermalization are observed [3, 7]. This makes them appropriate for their application as temperature sensor. This change is produced by a thermally induced population redistribution between two adjacent levels that are optically coupled to a lower common level. Moreover, those levels are thermally coupled due to the fact that they have a high probability of undergoing non-radiative transitions [8]. This effect could be characterized by means of the Fluorescence Intensity Ratio technique (FIR) and employed as a method for the temperature measurement. FIR technique is based on the comparison of the fluorescence intensities of two energy levels, with the constraint that they must lie close, as mentioned above [9]. The $^2H_{11/2}$ and $^4S_{3/2}$ levels of Er^{3+} ions are appropriate in order to use this method [6, 7].

If a material is doped with Nd^{3+} ions, it also experiences changes in the shapes of their thermalized emission bands when its temperature is changed. The $^4F_{3/2}$ and $^4F_{5/2}$ levels of Nd^{3+} ions are also adequate to apply the FIR technique [7].

Taking advantage of these facts, these ions have been employed to develop new temperature sensors in the last years [2, 7].

Going further with the idea of developing optical sensors for bio- and nanotechnological applications, researchers have tried to find sensors of the appropriate dimensions [10-12]. Thus began the studies in the use of microspheres as optical temperature sensors.

Microspheres are spherical transparent dielectric microcavities with diameters around micrometers, usually made of silica compounds. They must have higher refractive index than their enclosing medium in order to generate total internal reflection and, consequently, morphology-dependent resonances. Due to minimal reflection losses and to potentially very low material absorption, these resonators can reach exceptionally high-quality factors which lead to very high energy density [13]. Their spherical symmetry enables their use as resonant cavities, what produces the effect known as Whispering Gallery Modes (WGM).

WGM are yielded by electromagnetic waves confined inside a microsphere due to their reflections in its internal surface, which acts as resonator cavity. These reflections have minimal losses, so WGM reach high-quality factors and, consequently, very narrow resonant-wavelength lines [13]. Moreover, if the microsphere suffers a change in its temperature, this produces a change in its size and, consequently, this yields wavelength shifts of the WGM [5]. This result is the basis of the other method for the measurement of temperature shifts studied in this work. Others applications of WGM are reviewed in Ref. [14].

A Strontium Barium Niobate (SBN) glass sample, which was codoped with Er^{3+} and Yb^{3+} trivalent ions, was used as precursor glass so as to produce the microsphere employed in the first section of this work. This type of materials are transparent in the range of visible radiation, what makes them interesting for optical applications. Moreover, glassceramics can be obtained from these precursor glasses with the appropriate thermal treatment. These glassceramics have glassy and crystalline phases. The crystalline phase is formed by SBN nanocrystals, which have large pyroelectric and linear electro-optic coefficients, as well as strong photorefractive effects. They are ferroelectric materials, with Curie temperatures ranging from 320 to 470 K. Piezoelectric properties with large spontaneous polarization of this material are of great interest [7].

Taking advantage of the transfer processes from Er^{3+} to Yb^{3+} ions, the analysis of the dependence of WGM with temperature in the emission band of ytterbium has been enabled. WGM are very sensitive to the refractive index of the microsphere and size changes, which are caused by a shift in temperature [15]. The sensitivity with temperature of this method is compared with the one of FIR technique applied to the thermalized bands of Er^{3+} ions.

Under certain conditions, microspheres can produce the phenomenon termed a photonic nanojet. A photonic nanojet is a narrow, high-intensity, non-evanescent light beam with a waist under the Abbe diffraction limit. This nanojet can propagate over a distance longer than the excitation wavelength after emerging from the shadow-side surface of an illuminated lossless dielectric microsphere of diameter larger than the excitation wavelength. Photonic nanojets have applications for detecting and manipulating nanoscale objects, subdiffraction-resolution nanopatterning and nanolithography, low-loss waveguiding (WGM above explained) and ultrahigh-density optical storage, among others [16]. Moreover, this phenomenon makes possible the use of microspheres as lenses which collect light beams concentrating them in the photonic nanojet [17, 18]. Thus, it is possible to heat a specific and small area. Moreover, this

punctual heating has interesting potential applications in biotechnology [1] and also in some branches of nanotechnology [16].

The last part of this study consists in the analysis of the optical properties of a Nd^{3+} doped phosphate glass. These phosphate glasses are of great interest due to their frequent applications in the field of optical transmission, detection, sensing and laser technologies [19]. Phosphate glasses show unique characteristics such as a great solubility of lanthanide trivalent ions, low linear and nonlinear refractive index, high transparency, low melting point, good thermal stability, low dispersion and high gain density [20]. Therefore, their emission properties as function of the Nd^{3+} concentration have been analysed in this work in order to obtain the maximum possible emission optimizing its concentration.

With the above mentioned aim, the energy transfer processes which take place in the studied bulks were analysed. As the concentration of ions grows, the distance between them decreases. As a consequence, the interaction between them increases. Therefore, non-radiative energy transfer processes between doping ions are more likely to happen. When the migration processes between donor ions are important, the model proposed by Parent is used [21]. This model includes the Inokuti-Hirayama model as a particular case [22], in which the migration between donor ions is not considered [23].

Methodology

Los materiales analizados en este trabajo fueron dopados con iones lantánidos con niveles termalizados. Para caracterizarlos se tomaron espectros de emisión para una serie de temperaturas y se analizaron con la técnica FIR. Los resultados obtenidos para el valor del gap de los niveles termalizados se compararon con los obtenidos de las medidas de absorción. Se tomaron espectros de emisión variando la potencia de la excitación. A partir de los resultados obtenidos se calculó la sensibilidad de la termalización de los niveles y del desplazamiento de los modos de resonancia con la temperatura. Además, para el estudio de los procesos de transferencia de energía se tomaron medidas del decaimiento de la intensidad. Estos datos se ajustaron al modelo de Parent o al de Inokuti-Hirayama según se considerara o no la posibilidad de migración entre donores.

Experimental procedures

The SBN precursor glass was obtained with the following composition in mol %: 4 Yb_2O_3, 0.1 Er_2O_3, 11.25 SrO, 11.25 BaO, 22.5 Nb_2O_5 and 50.9 B_2O_3. It was prepared by a standard melt quenching method. Commercial powders of reagent grade were mixed and melted in a platinum crucible in an electric furnace at 1400 ºC for one hour. The melt was poured between two iron plates and the thickness of the obtained sample was 1.0 mm.

A set of measurements of the refractive index of this bulk for different wavelenghts in the visible region were done and fitted to the Cauchy equation. It was obtained a value of 2.0 refractive index in the range of wavelength of interest for the analysis of WGM.

The alteration of the emission spectrum of the SBN glass as a function of temperature was studied in the 280-580 K range employing a furnace and exciting the sample at 488 nm with an Argon laser as it was done in Refs. [3, 4].

The absorption spectrum of the SBN bulk in the range from 450 to 650 nm was measured with the spectrophotometer Cary 5000 in order to obtain the value of the energy mismatch between the thermally coupled levels of erbium, denoted by E_{32}.

The microspheres were prepared by the method of rapid quenching of liquid droplets exposed by G.R. Elliot et al. [24] from the precursor glass mentioned above. Using this technique, microspheres of diameters ranging from 10 to 100 μm were produced. In this study, a sphere of approximately 40 μm of diameter was employed.

The emission spectra of this Er^{3+}-Yb^{3+} codoped microsphere in the range from 700 to 1100 nm were obtained exciting at 532 nm with a commercial continuous wave Diode Pumped Solid State Laser and using a modified confocal microscope as was indicated in Ref. [25].

The neodymium doped materials are a set of phosphate glasses with the following composition in mol %: 44 P_2O_5, 17 K_2O, 9 Al_2O_3, (30-x) CaF_2 and x Nd_2O_3, where x =0.1, 0.5, 1.0 and 2.0 mol %. These glasses were prepared by a standard melt quenching method.

The emission spectra of the 2 mol % of Nd^{3+} doped glass for diverse temperatures in the 300-520 K range where taken using a furnace and exciting the sample at 532 nm by means of a Diode Laser, similarly to the procedure in Refs. [3, 4].

The microspheres employed as focusing lens are made of silica by the Bangs Laboratories, Inc. Spheres of 2, 7 and 25 μm of diameter were chosen.

The emission spectra of the neodymium doped bulk glass with a microsphere acting as a focusing lens were obtained exciting at 532 nm with a commercial continuous wave Diode Pumped Solid State Laser and employing a microscope as was indicated in Ref. [17].

The intensity decay measurements were taken exciting the diverse neodymium doped samples at 532 nm by means of a pulsed Nd: YAG laser and detecting with a TRIAX 180 monochromator and a photomultiplier tube.

The absorption spectrum of the 2 mol % neodymium doped glass in the range from 750 to 950 nm was measured with the spectrophotometer Cary 5000 so as to obtain the value of the energy mismatch between the thermally coupled levels of neodymium, E_{32}.

Theoretical models

Fluorescence intensity ratio technique

With the aim of characterizing the heating effect in the thermalized bands of erbium and neodymium, the fluorescence intensity ratio technique (FIR) has been employed. This technique compares the fluorescence intensities of two adjacent thermalized energy levels, which are in thermal equilibrium and optically coupled to a lower common level. These levels are thermally coupled due to the fact that they have a high probability of undergoing non-radiative transitions [8]. As the emitted intensities are proportional to their respective populations, the parameter called fluorescence intensity ratio, R, results

$$R = \frac{I_{31}}{I_{21}} = \frac{\omega_{31}^{R} g_3 h\nu_3}{\omega_{21}^{R} g_2 h\nu_2} exp\left(-\frac{E_{32}}{k_B T}\right) \quad (1)$$

where k_B is the Boltzmann constant, g_3 and g_2 are the degeneracies *(2J+1)* of these levels and ω^R_{31} and ω^R_{21} are the spontaneous emission rates of the E_3 and E_2 levels to the E_1 level, respectively [9].

This thermally induced population redistribution between the two adjacent levels follows a Boltzmann-type behaviour, as can be seen in Eq. (1).

Sensitivity

A commonly used parameter employed to characterize optical temperature sensors is the sensitivity, S, which represents the variation of the measured parameter with the temperature relative to its magnitude.

The sensitivity for the parameter R, the ratio obtained by the FIR technique, is given by the following expression [5, 8]

$$S_{FIR} = \frac{\delta R}{R\ \delta T} = \frac{E_{32}}{k_B T^2} \quad (2)$$

In the same way, the sensitivity for the displacement of the WGM with temperature results

$$S_{WGM} = \frac{\delta \lambda}{\lambda\ \delta T} \quad (3)$$

Energy transfer processes

Interaction processes between optically active ions appear if their concentration increases. This is due to the fact that the mean distance between the interacting ions decreases, which would cause that energy transfer processes were appreciable.

Considering non-radiative energy transfer processes, were photons are not involved, and a multipolar interaction between the neodymium trivalent ions as the predominant interaction, the temporal evolution of the emission after the excitation pulse, *I(t)*, should obey the following models.

Inokuti-Hirayama model. When migration among donors is not considered, the temporal evolution of the emitted intensity, *I(t)*, is described by Inokuti and Hirayama in Ref. [23] as

$$I(t) = I(0)\ exp\left[-\frac{t}{\tau} - Q\left(\frac{t}{\tau}\right)^{3/S}\right] \quad (4)$$

where *I(0)* is the intensity at time t=0; τ is the intrinsic lifetime of the engaged donor level; *S* depends of the type of interaction (for dipole-dipole interaction, *S*=6) and, if there is only a type of acceptor ion, *Q* is given by

$$Q = \frac{4\pi}{3}\Gamma\left(1-\frac{3}{S}\right)A(C_{DA}\tau)^{3/S} \tag{5}$$

where Γ is the gamma function, A is the concentration of ions and C_{DA} is the donor-acceptor energy transfer parameter.

The dependence of the emitted intensity, *I*, on the concentration of doping ions, A, is given by [22]

$$I \propto N^* = \frac{6\phi A}{\frac{1}{\tau}+W_T} \tag{6}$$

where ϕ is the flow of photons per cm^2 and W_T is the transfer probability, that can be calculated using

$$W_T = \frac{\eta_T}{\tau(1-\eta_T)} \tag{7}$$

where η_T is the transfer efficiency.

This model allows to obtain the transfer efficiency for dipole-dipole interaction from [22]

$$\eta_T = \sqrt{\pi}\, x\, exp(x^2)\,[1-erf(x)] \tag{8}$$

where *erf(x)* is the error function and *x* is given by

$$x = \frac{2\pi}{3}\sqrt{\pi}\, A\, {C_{DA}}^{1/2}\, \tau^{1/2} \tag{9}$$

Moreover, considering Eq. (5) for the case S=6, *x* can be expressed in terms of Q as

$$x = \frac{Q}{2} \tag{10}$$

Parent model. When the migration processes among donors are important, the model proposed by Parent [21] would be used instead of the one expounded previously. The dependence for I(t) if S=6 is given by

$$I(t) = I(0)\, exp\left[-\frac{t}{\tau} - Q\left(\frac{t}{\tau}\right)^{1/2} - W_D t\right] \tag{11}$$

where W_D is a probability that characterizes the migration processes and depends on C_{DA} and C_{DD}, the donor-donor energy transfer parameter.

According to the emitted intensity dependence on the concentration of doping ions described by Eq. (6), this model allows to obtain the transfer efficiency for dipole-dipole interaction from [22]

$$\eta_T{}' = \frac{\sqrt{\pi}\, x' exp\left(x'^2\right)\left[1 - erf(x')\right] + \tau W_D}{1 + \tau W_D} \tag{12}$$

where *x'* is given by

$$x' = \frac{2\pi}{3}\sqrt{\pi}\, A\, C_{DA}{}^{1/2} \left[\frac{\tau}{1 + \tau W_D}\right]^{1/2} \tag{13}$$

However, taking into account the Eq. (5) for S=6, *x'* can be obtained from Q as

$$x' = \frac{Q}{2\sqrt{1 + \tau W_D}} \tag{14}$$

As can be seen, Inokuti-Hirayama model for *S*=6 is included as a particular case into Parent model; if the migration between donors is negligible (W_D=*0*), Eq. (4), (8) and (9) are obtained from Eq. (11), (12) and (13), respectively [22].

Results

Las bandas de emisión del espectro del vidrio SBN dopado con Er^{3+} e Yb^{3+} excitado en 532 nm se identifican con las siguientes transiciones: $^2H_{11/2} \rightarrow {}^4I_{13/2}$ (800 nm) y $^4S_{3/2} \rightarrow {}^4I_{13/2}$ (855 nm) para el erbio y $^2F_{5/2} \rightarrow {}^2F_{7/2}$ (975 nm) para el yterbio. Se obtiene el gap de energía entre los niveles $^2H_{11/2}$ y $^4S_{3/2}$ del erbio (749 cm^{-1}). Se observan los modos de resonancia de la microesfera y se obtiene un desplazamiento medio de 9 pmK^{-1}. Utilizando las microesferas como lentes que concentran la radiación sobre la muestra, se concluye que la esfera de 2 μm de diámetro produce un calentamiento mayor que las esferas de mayores dimensiones. A partir de las medidas del decaimiento de la intensidad de las muestras de los vidrios de fosfato dopados con Nd^{3+}, con diferentes concentraciones, se obtiene el tiempo de vida intrínseco y el parámetro de transferencia de energía (Q) según la concentración. Además, se determina que la concentración óptima de iones de Nd^{3+} para lograr la máxima intensidad de emisión es 2.2 mol % de Nd^{3+}.

Temperature dependence of the whispering gallery modes

When the Er^{3+}–Yb^{3+} codoped SBN glass is excited under a 532 nm laser radiation, the spectrum plotted in Fig. 1b with a red line is obtained. As can be seen, it shows broad bands that correspond to typical transitions of Er^{3+} and Yb^{3+} ions in a glass matrix. These transitions can be easily assigned to the erbium $^2H_{11/2} \rightarrow {}^4I_{13/2}$ (800 nm) and $^4S_{3/2} \rightarrow {}^4I_{13/2}$ (855 nm). Moreover, the broad band observed at 975 nm is typical of Yb^{3+} ions, corresponding to the $^2F_{5/2} \rightarrow {}^2F_{7/2}$ transition. In this case, these ions are excited by energy transfer processes from Er^{3+} ions. These transitions are schematically shown in Fig. 1a.

A similar spectrum is obtained when the sample is a glass microsphere made of the same material. However, if the excitation is performed especially in the sphere centre and the detection is located near its border with the confocal microscope mentioned in the experimental section, sharp peaks appear due to the typical WGM (see Fig. 1b, blue line). This effect was also detected in microspheres of similar glasses with Nd^{3+} as doping ion [5].

The emission spectra measurements obtained in WGM configuration for different laser powers are shown in Fig. 2. As a consequence of the increase of the laser power, two important effects related with the heating of the microsphere are observed: the thermalization effect of the $^2H_{11/2}$ and $^4S_{3/2}$ erbium levels and the displacement of WGM peaks. These effects are discussed in detail in the following sections.

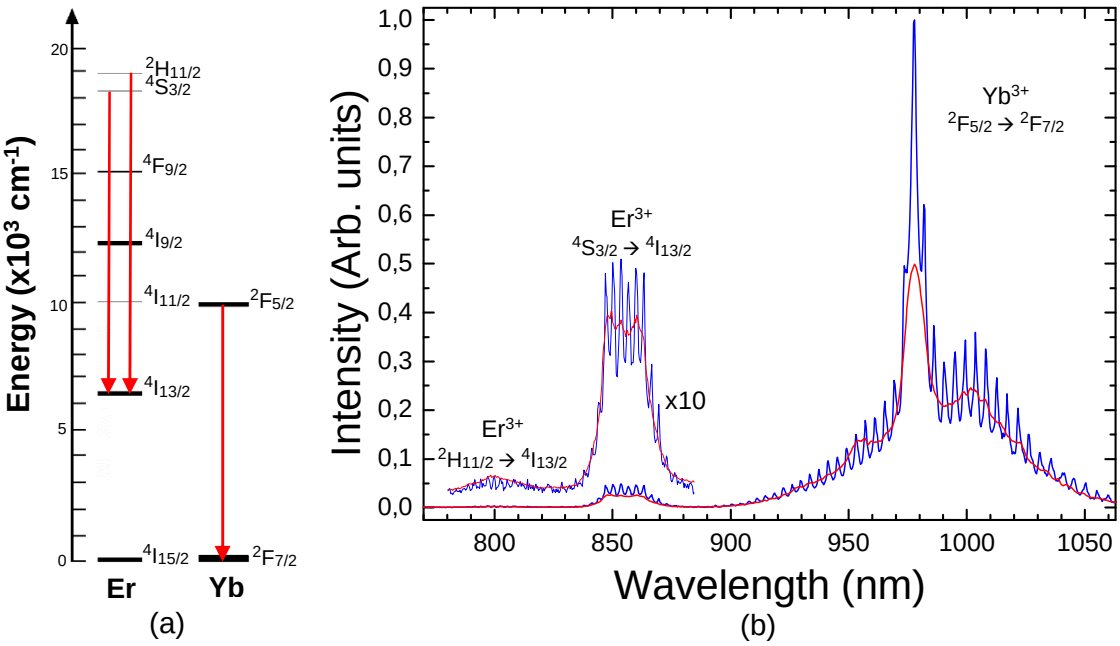

Fig. 1. (a) Energy-level diagram for erbium and ytterbium trivalent ions, where the transitions of interest are indicated. (b) Emission spectrum of the Yb^{3+}-Er^{3+} codoped glass obtained under excitation at 532 nm (red line). Emission spectrum of an Yb^{3+}-Er^{3+} codoped microsphere positioning the detection in the border of the sphere in order to observe the WGM under excitation at 532 nm (blue line). In the range from 780 to 885 nm, a x10 zoom of the spectra was made.

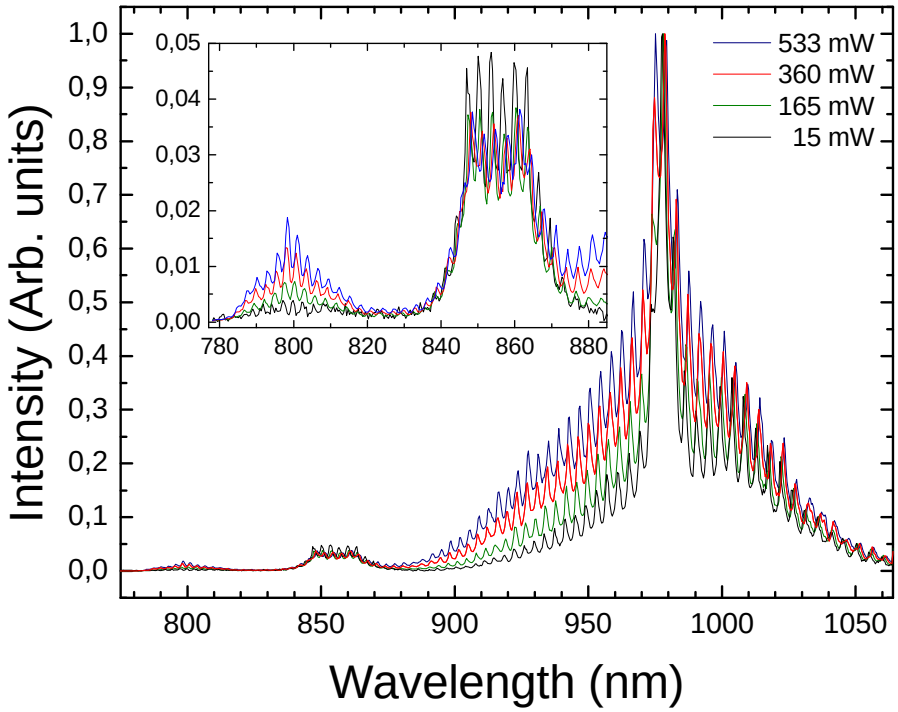

Fig. 2. Emission spectra of an Yb^{3+}-Er^{3+} codoped sphere under excitation at 532 nm, obtained for different laser powers. The inset graphic shows in detail the thermalized bands of the Er^{3+} ions ($^2H_{11/2}$→$^4I_{13/2}$ (800 nm) and $^4S_{3/2}$→$^4I_{13/2}$ (855 nm)) in the 780-880 nm range.

Thermalization effect in Er^{3+} ions

The $^2H_{11/2}$ and $^4S_{3/2}$ energy levels of Er^{3+} ions are very close to each other (with an energy mismatch of 749 cm^{-1}). Therefore, their populations follow a Boltzmann distribution law and, as consequence, the emission from these levels has the temperature dependence predicted by this law (Eq. (1)). As can be seen in the inset graphic of Fig. 2, when the laser power is increased, the areas of the $^2H_{11/2} \rightarrow {}^4I_{13/2}$ (800 nm) and $^4S_{3/2} \rightarrow {}^4I_{13/2}$ (855 nm) bands change differently, what could be due to the increase in temperature.

The experimental values for the fluorescence intensity ratio plotted in Fig. 3 are the result of a calibration process, which makes possible the connexion between the experimentally obtained ratio values and temperature. These data have been obtained from a bulk glass using the experimental setup described in the experimental section. The experimental values for the ratio have been fitted to Eq. (1), that is to say, FIR technique was applied. As can be seen in the Fig. 3, a good agreement with the expected behaviour has been obtained, with a value for E_{32}= 742 cm^{-1}, which is similar to the value previously obtained by means of the measurement of the absorption of this material (E_{32}=749 cm^{-1}).

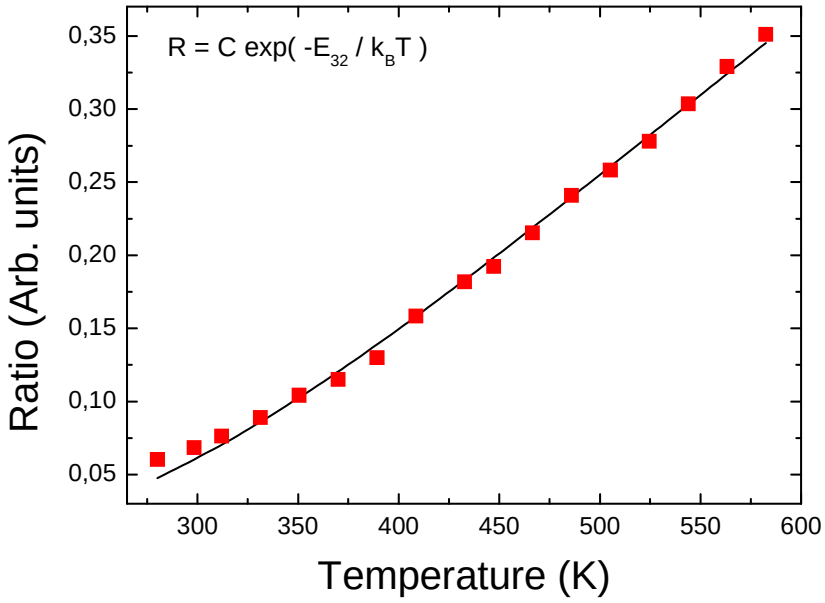

Fig. 3. Calibration of the variation of the ratio between the thermalized bands of Er^{3+} ions ($^2H_{11/2} \rightarrow {}^4I_{13/2}$ (800 nm) and $^4S_{3/2} \rightarrow {}^4I_{13/2}$ (855 nm)) with temperature (red squares). The solid line corresponds to the fitting to the Boltzmann equation (Eq. (1)).

By means of this calibration a temperature can be associated to the fluorescence intensity ratio value obtained for each measured spectrum of the Er^{3+} thermalized bands shown in Fig. 2. The corresponding results are plotted in Fig. 4.

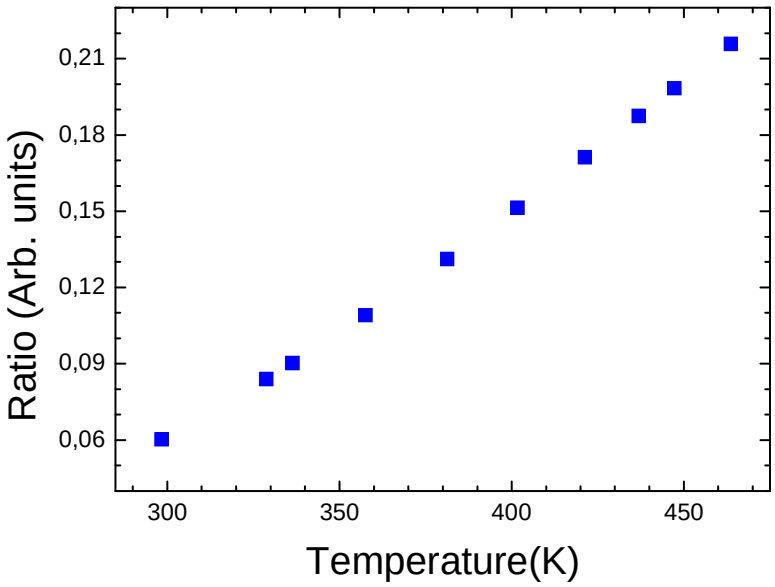

Fig. 4. Calculated ratio for the thermalized bands of Er^{3+} ($^2H_{11/2} \rightarrow {}^4I_{13/2}$ (800 nm) and $^4S_{3/2} \rightarrow {}^4I_{13/2}$ (855 nm)) as function of temperature, which is calculated using the previous calibration.

With the purpose of characterizing the response of the measured parameter R, obtained by the FIR technique, its sensitivity was calculated by means of Eq. (2). The results obtained for the sensitivity S_{FIR} are shown in Fig. 5.

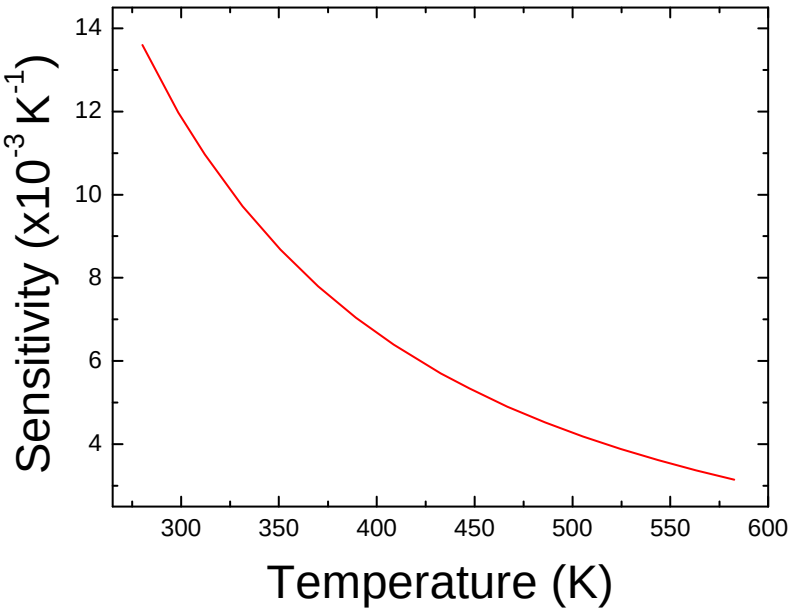

Fig. 5. Sensitivity for the parameter R obtained by the FIR technique, calculated using Eq. (2) for the temperature range of the calibration.

The sensitivity of the parameter R achieves its maximum value (S_{FIR} =1.36 10^{-2} K^{-1}) at the lowest temperature in the measured range.

Displacements of the Whispering Gallery Modes

The displacements of five different WGM due to the heating effect produced by the laser excitation are plotted in Fig. 6. The temperature has been calculated using the previous fit to Eq. (1) of the ratio of the thermalized bands of Er^{3+} ions. Due to the heating of the sphere, its volume increases and, as a consequence of the shift in the dimensions of the resonator cavity, the wavelengths of the WGM change. Therefore, it is expected the red-shift of the wavelength for the WGM shown in Fig. 6.

From the measurement of the displacements in wavelength of the maxima of five whispering peaks with the shift in temperature it was be obtained an averaged displacement of 9 pm/K.

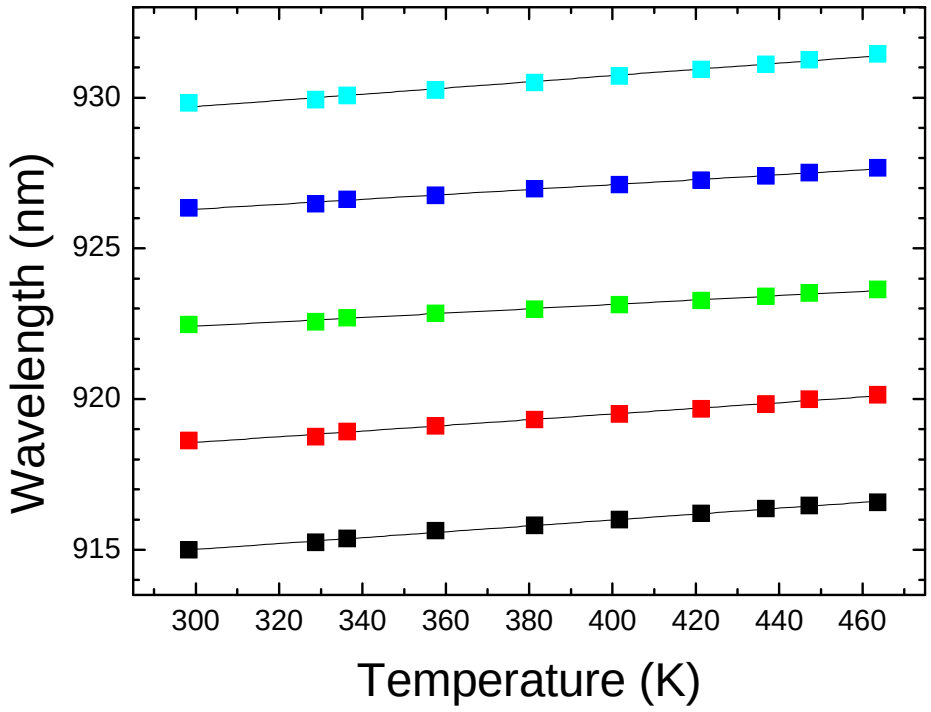

Fig. 6. Displacements of five WGM of an Yb^{3+}-Er^{3+} codoped microsphere as function of the temperature.

This result could be considered as a characterization of the sensitivity of this method in order to be used as temperature sensor. However, with the aim of comparing

this method with the one previously discussed, the sensitivity of the wavelength displacement in WGM was obtained through Eq. (3). The results are shown in Fig. 7.

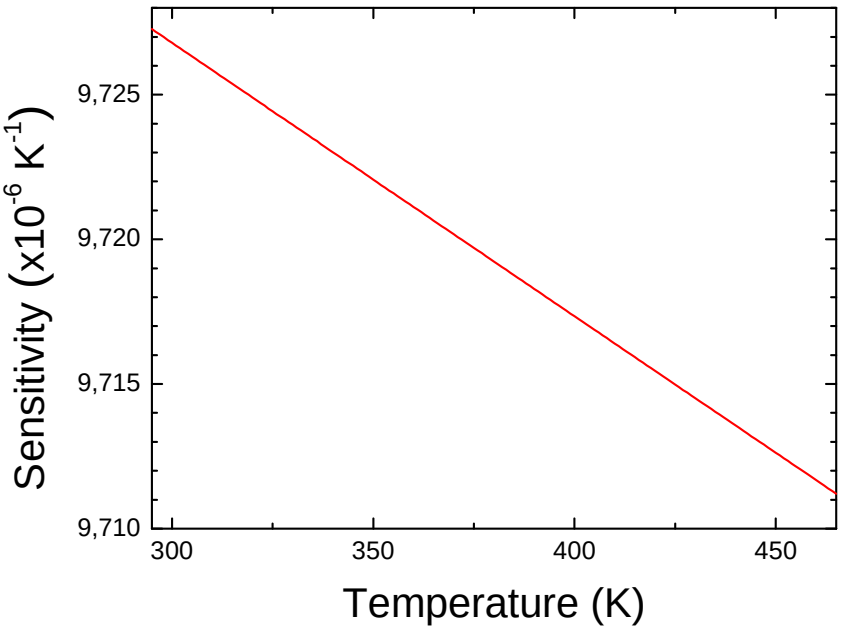

Fig. 7. Sensitivity for the displacement of the wavelength of the WGM, calculated using Eq. (3) in the 295 – 465 K range.

The maximum value for the sensitivity of the displacement of the WGM (S_{WGM}=9.727 10^{-6} K^{-1}) is found for the lowest temperature in the studied range, in similar way to S_{FIR}.

The sensitivity obtained for the FIR ratio yields a temperature resolution limit about 1 K [5]. However, according to Ref. [10], WGM can reach quality factors of 10^5 and the limit of detection of the WGM is about 1 % of the line-width of the resonance. Thus, the limit of resolution in temperature of this method is about 0.01 K, that is to say, this method enables a resolution limit in temperature two orders of magnitude higher than FIR technique. In conclusion, WGM allow a finer temperature estimation [5].

A similar study about the dependence of WGM with temperature was done in Ref. [5] for a Nd^{3+} doped barium titano silicate glass. However, the use of an Er^{3+}-Yb^{3+} doped sample gives more options. For instance, it allows the observation of WGM in a wider spectral range due to the emissions of erbium and ytterbium ions. Moreover, ytterbium is more efficient than other lanthanides, due to the fact that it has only two energy levels with a wide mismatch. In future works, this sample would enable to observe at the same time WGM and upconversion processes.

Heating using a microsphere as a focusing lens

Silica microspheres were deposited over a 2 mol % Nd^{3+} doped phosphate glass, in order to concentrate the incident light over the bulk [17]. The spectra plotted in Fig. 8a have been obtained excited under a 532 nm laser radiation. As can be observed, they show broad bands that correspond to typical transitions of Nd^{3+} ions in a glass matrix. These bands can be easily identified as $^4F_{3/2} \rightarrow {}^4I_{9/2}$ (800 nm) and $^4F_{5/2} \rightarrow {}^4I_{9/2}$ (880 nm) transitions (see Fig. 8b). This emission spectra were obtained using microspheres of 2, 7 and 25 µm diameter under the same experimental conditions (Fig. 8a). This procedure enables to know which one of these spheres yields the highest ratio value for the thermalized bands, that is to say, which one produces the highest heating by the nanojet.

The $^4F_{3/2}$ and $^4F_{5/2}$ energy levels of neodymium ions are very close (see Fig. 8b), with an energy mismatch about 1054 cm^{-1}, obtained from the absorption spectrum. Therefore, their populations follow a Boltzmann distribution law and the emission from these levels is in accordance with the temperature dependence predicted by this law (Eq. (1)). Consequently, when the temperature is increased, the ratio between the $^4F_{3/2} \rightarrow {}^4I_{9/2}$ (800 nm) and the $^4F_{5/2} \rightarrow {}^4I_{9/2}$ (880 nm) bands changes [4].

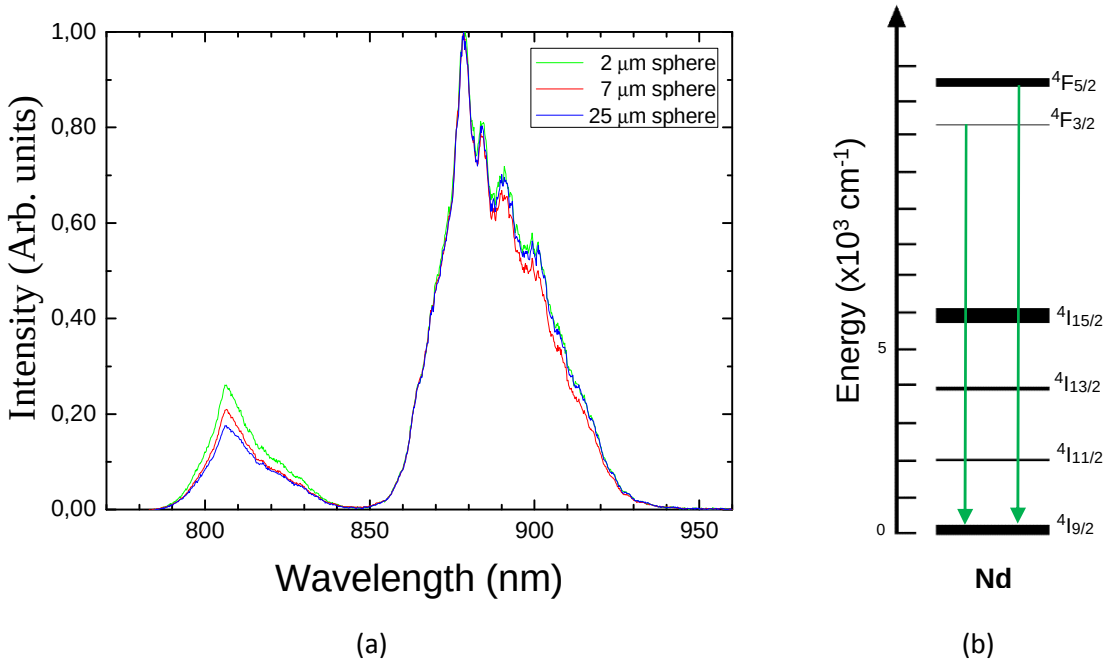

Fig. 8. (a) Spectra of thermalized bands of 2 mol % Nd^{3+} doped bulk glass excited at 532 and using spheres of diverse diameters acting as lenses. (b) Energy-level diagram for neodymium trivalent ions, where the transitions of interest are indicated.

In order to calibrate the ratio with the temperature, the emission spectra of a bulk glass located inside of a furnace has been measured. The experimental values for the

ratio, plotted in Fig. 9, have been fitted to Eq. (1), as the FIR technique specifies. A good concordance has been obtained with an E_{32}= 1088 cm^{-1}, which is similar to the result obtained by absorption (1054 cm^{-1}).

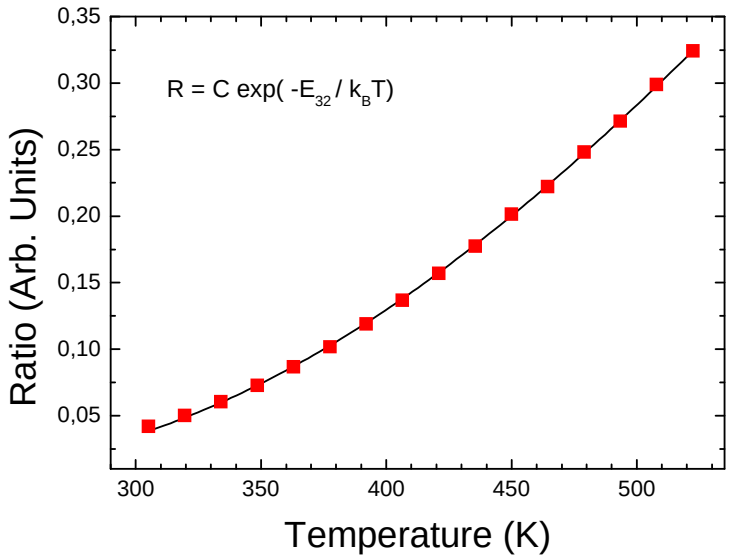

Fig. 9. Calibration of the variation of the ratio between the thermalized bands of Nd^{3+} ions with temperature (red squares). The experimental data have been fitted to Boltzmann equation (Eq. (1)) (black line).

Once FIR technique is applied to the spectra of Fig. 8a, the sphere of 2 μm of diameter came out being the better to produce a higher increase of temperature in the focalized zone, as can be observed in Fig. 10.

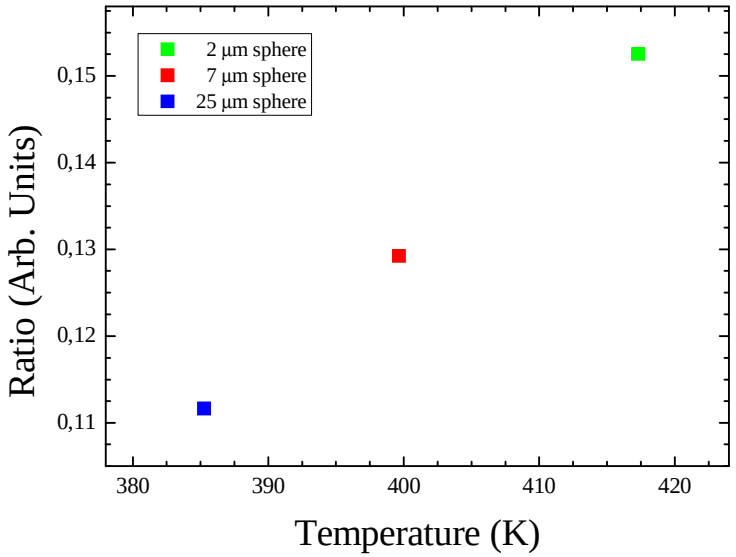

Fig. 10. Calculated ratio, by means of FIR technique, for the thermalized bands of spectra in Fig. 8a.

As a consequence of this result, measurements of the spectrum for the sphere of 2 µm were done for a series of increasing values of laser power, from 80 to 790 mW. The results, calculated by means of FIR technique, are shown in Fig. 11. The corresponding temperature for each laser power has been calculated using the calibration above expounded. Therefore, it has been possible to increment 110 K the temperature of the focalised region using the photonic nanojet.

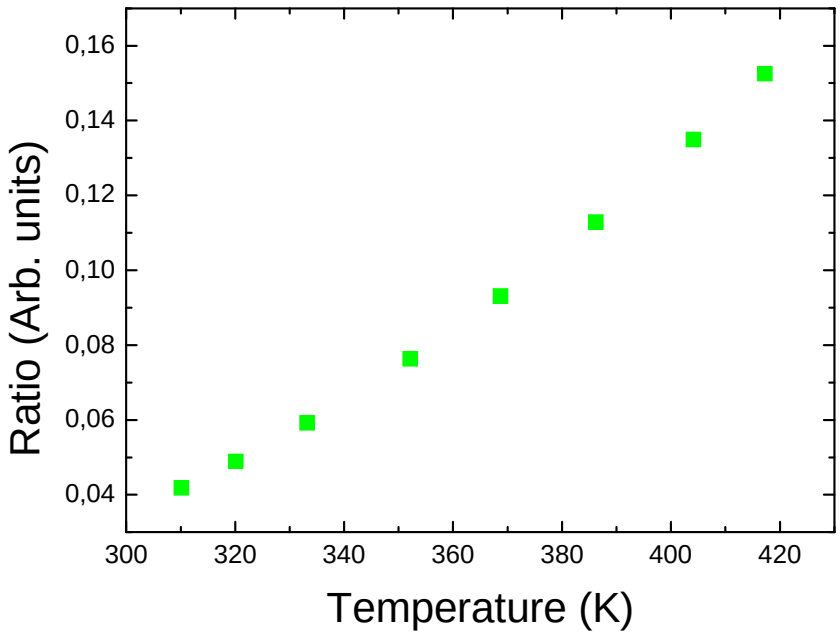

Fig. 11. Ratio, calculated by means of FIR technique, for a set of measurements, varying the laser power from 80 to 790 mW, of the 2 mol % Nd^{3+} doped bulk thermalized bands spectrum with the 2 µm diameter sphere acting as lens. Temperature was calculated using the calibration of the bulk (Fig. 9).

Determination of the optimum concentration of doping ion

Firstly, intensity decay measurements for the bulks with diverse concentrations of doping ions were taken exciting at 532 nm and detecting the dispersed radiation emitted spontaneously by the sample (see Fig. 12). The intrinsic lifetime (τ=0.34 ms) was obtained by the fitting of the intensity decay curve of the bulk with the lowest concentration of Nd^{3+} ions to the expected exponential behaviour. This bulk is suitable for this purpose due to the fact that a low concentration implies that the probability of energy transfer processes between the ions is negligible, as explained above.

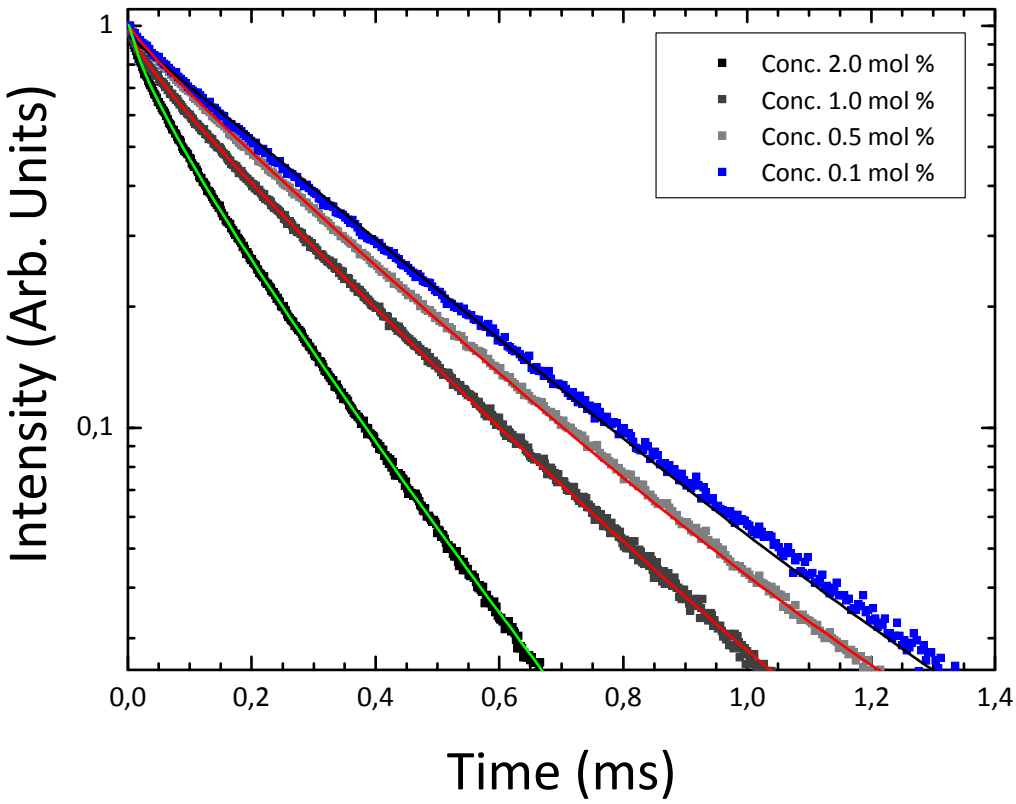

Fig. 12. Temporal evolution decays obtained for different Nd^{3+} doped glasses with diverse concentrations in mol % of Nd^{3+}. Fit to an exponential decay (black line), fit to Inokuti-Hirayama model (red lines) and fit to Parent model (green line).

Once the intrinsic lifetime was obtained, the decays for bulks with higher concentrations could be fitted to the corresponding theoretical model above expounded. The bulks of medium concentrations were well fitted to Inokuti-Hirayama model, taking into account that the energy transfer processes begin to be appreciable for higher values of A. The results for the energy transfer parameter Q were 0.22 and 0.43 for the concentrations of 0.5 and 1.0 mol %, respectively. The bulk with the highest concentration was fitted to Parent model, due to the fact that the energy transfer processes among donors (migration processes) are important in this case. The following values for the energy transfer parameter and the probability of migration processes were obtained for the 2.0 mol % doped sample: Q=0.82 and W_D=0.96 s^{-1}.

As can be observed in Fig. 13, where the results obtained for Q in the previous fittings are shown, they have a linear dependence with A, the concentration of doping ions, as predicted by Eq. (5). From this fit, the donor-acceptor energy transfer parameter was calculated, obtaining C_{DA}=1.2 10^{-40} cm^6s^{-1}, which is similar to the value obtained in Ref. [26] in other matrix.

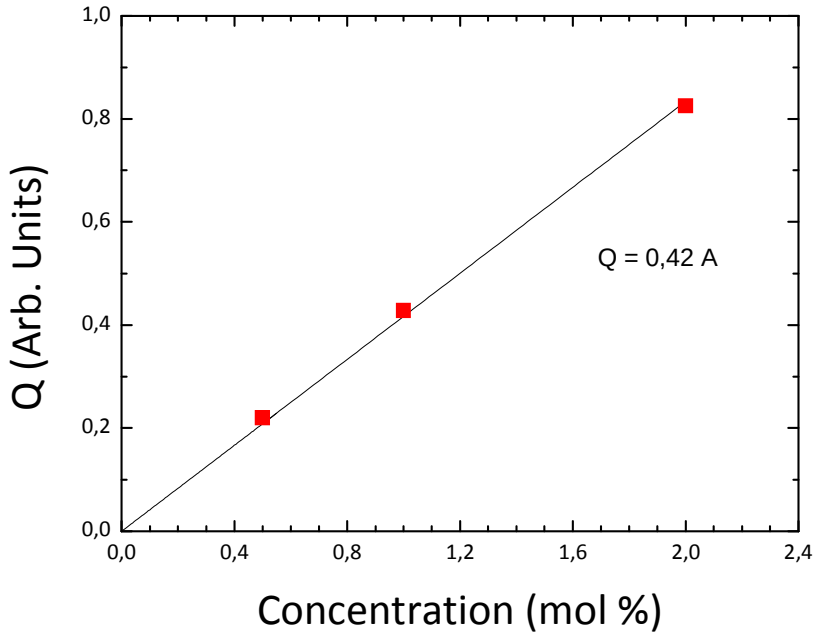

Fig. 13. Values for the energy transfer parameter Q (red squares) obtained with the fits to the decay curves shown in Fig. 12. A fit to the expected linear expected behaviour has also been represented (black line) according to Eq. (5).

Using relations given by Eq. (10) and Eq. (14), the transfer efficiency for both models (Eq. (8) and Eq. (12)) can be calculated, respectively. Consequently, the corresponding transfer probability is obtained by means of Eq. (7). This result enables calculating the intensity associated to a given doping ion concentration according to each of these models using Eq. (6), which is shown in Fig. 14.

In order to characterize the suitability of theses theoretical calculations with experimental results, some measurements of the intensity emitted by the bulks with diverse concentrations were made in the same conditions (see Fig. 14).

As can be observed in Fig. 14, there is a good agreement between the experimental data and the behaviour predicted by Parent model. According to this model, the neodymium optimum concentration so as to obtain the maximum intensity is 2.2 mol %. However, although Inokuti-Hirayama model is equally appropriate for not high concentrations, it overestimates the ratio values for the most concentrated sample, because it does not consider energy transfer processes between donor ions. Thus, the optimum concentration given by Inokuti-Hirayama model is not plausible.

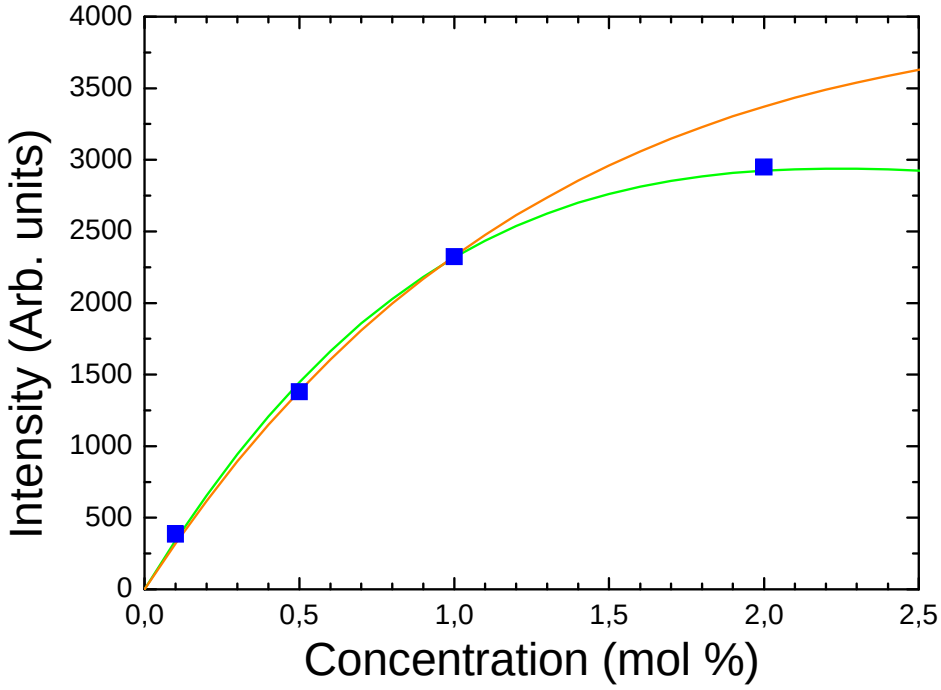

Fig. 14. Measurements of the emitted intensity for the different bulks under the same conditions (blue squares), intensity calculated according to Inokuti-Hirayama model as a function of the concentration of doping ions (orange line) and intensity calculated according to Parent model as a function of the concentration of doping ions (green line).

Conclusions

Los resultados obtenidos indican que el desplazamiento de los modos de resonancia es el parámetro más apropiado para ser usado como sensor óptico de temperatura. Además, se concluyó que la esfera de 2 μm de diámetro produce un mayor calentamiento. Finalmente, se obtuvo una concentración óptima de Nd^{3+} de 2.2 mol %.

The transitions corresponding to the thermalized levels of erbium ions were identified as $^2H_{11/2} \rightarrow {}^4I_{13/2}$ (800 nm) and $^4S_{3/2} \rightarrow {}^4I_{13/2}$ (855 nm). These levels were found suitable for the application of the Fluorescence Intensity Ratio technique due to the fact that their population redistribution follows Boltzmann's law. Moreover, the results obtained for the energy mismatch of these levels by absorption (E_{32}=749 cm^{-1}) and by means of the fit to a Boltzmann distribution (E_{32}= 742 cm^{-1}) are in excellent agreement. The broad band at 975 nm, corresponding to the emission of Yb^{3+} ions excited by energy transfer processes from Er^{3+} ions, was identified with the $^2F_{5/2} \rightarrow {}^2F_{7/2}$ transition of ytterbium ions.

In this work, the observation of whispering gallery modes was achieved placing the detection in the border of the sphere. The effects of the heating in the microsphere with the laser power excitation at 532 nm were studied. The variation of the ratio between the thermalized levels of erbium was characterized and a maximum sensitivity of S_{FIR} =1.36 10^{-2} K^{-1} was found. At the same time, the displacement of the whispering gallery modes was observed, yielding a mean displacement of 9 pmK^{-1} and a maximum sensitivity of S_{WGM}=9.727 10^{-6} K^{-1}.

With the aim of studying the displacement of the whispering gallery modes in depth, an identification of the modes should have been done. For this purpose, the dilatation coefficient and the variation of the refractive index with temperature would be needed. Moreover, transverse magnetic and electric modes should have been differentiated during the adquisition of the spectra modifying the existing setup.

The transitions from thermalized levels of neodymium were also identified as $^4F_{3/2} \rightarrow {}^4I_{9/2}$ (800 nm) and $^4F_{5/2} \rightarrow {}^4I_{9/2}$ (880 nm). As a result of the fact that their population redistribution follows Boltzmann's law, these levels were found suitable for the application of the Fluorescence Intensity Ratio technique. Moreover, the results obtained for the energy mismatch of these levels by absorption (E_{32}=1054 cm^{-1}) and by means of the fit to a Boltzmann distribution (E_{32}= 1088 cm^{-1}) are in good agreement.

It was determined, by means of the Fluorescence Intensity Ratio technique, that the microsphere of 2 μm of diameter concentrates more the light that those of bigger dimensions (7 μm and 25 μm) analysed and, consequently, heats more in the zone of the nanojet.

The intrinsic lifetime of Nd^{3+} ions was obtained (τ=0.34 ms). From the fit to the corresponding theoretical models, according to the concentration of neodymium, the following results for the energy transfer parameter were obtained: Q=0.22, Q=0.43 and Q=0.82 for the concentrations of 0.5, 1.0 and 2.0 mol %, respectively. These Q results are proportional to the concentration of doping ions, as expected. The probability of migration processes given by the fit of the 2.0 mol % Nd^{3+} doped sample decay to Parent model was W_D=0.96 s^{-1}. The donor-acceptor energy transfer parameter was calculated, obtaining C_{DA}=1.2 10^{-40} $cm^6s\text{-}^1$.

The intensity associated to a given doping ion concentration according to each one of the models employed was calculated from the fit of Q. It was observed that the calculations done from Parent model were in good agreement with the experimental measurements independently of the concentration of Nd^{3+} ions. Inokuti-Hirayama model fits excellently to the experimental measurements of low and medium concentrations, but this model overestimate the intensity for high concentrations. This is in concordance with the fact that Inokuti-Hirayama model can be considered as a particular case of Parent model for negligible probability of migration processes. As conclusion, the estimated neodymium optimum concentration is 2.2 mol %.

References

1. J.-C.G. Bünzli. “Lanthanide Luminescence for Biomedical Analyses and Imaging.” Chemical Reviews. 110, 2729–2755 (2010).

2. D. Jaque and F. Vetrone. “Luminescence nanothermometry.” Nanoscale. 4, 4301–4326 (2012).

3. N. Vijaya, P. Babu, V. Venkatramu, C.K. Jayasankar, S.F. León-Luis, U.R. Rodríguez-Mendoza, I.R. Martín and V. Lavín. “Optical characterization of Er^{3+}-doped zinc fluorophosphate glasses for optical temperature sensors.” Sensors and Actuators B: Chemical. 186, 156–164 (2013).

4. C. Pérez-Rodrìguez, L.L. Martín, S.F. León-Luis, I.R. Martín, K.K. Kumar and C.K. Jayasankar. “Relevance of radiative transfer processes on Nd^{3+} doped phosphate glasses for temperature sensing by means of the Fluorescence Intensity Ratio technique.” Sensors and Actuators B: Chemical. (2014).

5. L. L. Martín, C. Pérez-Rodríguez, P. Haro-González, and I. R. Martín. “Whispering gallery modes in a glass microsphere as a function of temperature.” Optics express. Vol. 19, No. 25 (2011).

6. J.M. Ward and S.N. Chormaic. “Thermo-optical tuning of whispering gallery modes in Er:Yb co-doped phosphate glass microspheres.” Applied Physics B. Vol. 100, 847-850 (2010).

7. P. Haro-González, I.R. Martín, L.L. Martín, S. F. León-Luis, C. Pérez-Rodríguez and V. Lavín. “Characterization of Er^{3+} and Nd^{3+} doped Strontium Barium Niobate glass ceramic as temperature sensors.” Optical Materials. Vol. 33, Issue 5, P. 742–745 (2011).

8. V. K. Rai. “Temperature sensors and optical sensors,” Applied Physics. B 88(2), 297–303 (2007).

9. S.A. Wade, S.F. Collins, and G.W. Baxter. “Fluorescence intensity ratio technique for optical fiber point temperature sensing.” Journal of Applied Physics. 94(8), 4743–4756 (2003).

10. F. Vollmer and S. Arnold. “Whispering-gallery-mode biosensing: label-free detection down to single molecules.” Nature Methods. Vol. 5, No. 7, 591-596 (2008).

11. F. Vollmer, S. Arnold, D. Braun, I. Teraoka and A. Libchaber. “Multiplexed DNA Quantification by Spectroscopic Shift of Two Microsphere Cavities.” Biophysical Journal. Vol. 85, Issue 3, P. 1974–1979 (2003).

12. F. Vollmer, S. Arnold and D. Keng. “Single virus detection from the reactive shift of a whispering-gallery mode.” Proceedings of the National Academy of Sciences of The United States of America. Vol. 105, N. 52, P. 20701-20704 (2008).

13. G. C. Righini, Y. Dumeige, P. Feron, M. Ferrari, G. Nunzi Conti, D. Ristic and S. Soria. “Whispering gallery mode microresonators: Fundamentals and applications.” Rivista del Nuovo Cimento. Vol. 34, N. 7 (2011).

14. A.B. Matsko, A.A. Savchenkov, D. Strekalov, V.S. Ilchenko, and L. Maleki. “Review of Applications of Whispering-Gallery Mode Resonators in Photonics and Nonlinear Optics.” IPN Progress Report. 42-162 (2005).

15. L.L. Martin, S.F. León-Luis, C. Pérez-Rodríguez, I.R. Martín, U.R. Rodríguez-Mendoza and V. Lavín. “High pressure tuning of whispering gallery mode resonances in a neodymium-doped glass microsphere.” Journal of the Optical Society of America B. Vol. 30, No. 12 (2013).

16. A. Heifetz, S.C. Kong, A.V. Sahakian, A. Taflove, and V. Backman. “Photonic Nanojets.” Journal of Computational and Theoretical Nanoscience. 6(9), 1979–1992 (2009).

17. C. Pérez-Rodríguez, S. Ríos, I.R. Martín, L.L. Martín, P. Haro-González and D. Jaque. “Upconversion emission obtained in Yb^{3+}-Er^{3+} doped fluoroindate glasses using silica microspheres as focusing lens.” Optics Express. Vol. 21, No. 9 (2013).

18. D. Gérard, A. Devilez, H. Aouani, B. Stout, N. Bonod, J. Wenger, E. Popov, and H. Rigneault. “Efficient excitation and collection of single-molecule fluorescence close to a dielectric microsphere.” Journal of the Optical Society of America B. 26(7), 1473–1478 (2009).

19. J.H. Campbell and T.I. Suratwala. “Nd-doped phosphate glasses for high-energy/high-peak-power lasers.” Journal of Non-Crystalline Solids. Vol. 263–264, P. 318–341 (2000).

20. T.I. Suratwala, R.A. Steele, G.D. Wilke, J.H. Campbell and K. Takeuchi. “Effects of OH content, water vapor pressure, and temperature on sub-critical crack growth in phosphate glass.” Journal of Non-Crystalline Solids. Vol. 263–264, P. 213–227 (2000).

21. C. Parent, C. Lurin, G. Le Flem and P. Hagenmuller. “$Nd^{3+} \rightarrow Yb^{3+}$ energy transfer in glasses with composition close to $LiLnP_4O_{12}$ metaphosphate (Ln = La, Nd, Yb).” Journal of Luminescence. Vol. 36, Issue 1, P. 49–55 (1986).

22. I.R. Martin, J. Mendez-Ramos, V.D. Rodriguez, J.J. Romero and J. Garcia-Sole. “Increase of the 800 nm excited Tm3+ blue upconversion emission in fluoroindate glasses by codoping with Yb3+ ions.” Optical Materials. Vol. 22, N. 4, P. 327-333 (2003).

23. M. Inokuti and F. Hirayama. “Influence of Energy Transfer by the Exchange Mechanism on Donor Luminescence.” The Journal of Chemical Physics. 43, 1978 (1965).

24. G.R. Elliott, D.W. Hewak, G.S. Murugan and J.S. Wilkinson. “Chalcogenide glass microspheres; their production, characterization and potential.” Optics Express. Vol. 15(26), P. 17542-17553 (2007).

25. P. Haro-González, I.R. Martín, and A. Hernández-Creus. “Nanocrystals distribution inside the writing lines in a glass matrix using Argon laser irradiation.” Optics Express. Vol. 18, Issue 2, P. 582-590 (2010).

26. B. Shanmugavelu, V. Venkatramu and V.V. Ravi Kanth Kumar. “Optical properties of Nd^{3+} doped bismuth zinc borate glasses.” Spectrochimica Acta Part A: Molecular and Biomolecular Spectroscopy. Vol. 122, P. 422 – 427 (2014).